

Provided for non-commercial research and education use.
Not for reproduction, distribution or commercial use.



This article appeared in a journal published by Elsevier. The attached copy is furnished to the author for internal non-commercial research and education use, including for instruction at the authors institution and sharing with colleagues.

Other uses, including reproduction and distribution, or selling or licensing copies, or posting to personal, institutional or third party websites are prohibited.

In most cases authors are permitted to post their version of the article (e.g. in Word or Tex form) to their personal website or institutional repository. Authors requiring further information regarding Elsevier's archiving and manuscript policies are encouraged to visit:

<http://www.elsevier.com/copyright>



Contents lists available at ScienceDirect

Journal of African Earth Sciences

journal homepage: www.elsevier.com/locate/jafrearsci

The provenance and tectonic setting of the Neoproterozoic Um Hassa Greywacke Member, Wadi Hammamat area, Egypt: Evidence from petrography and geochemistry

Yasser Abd El-Rahman^{a,b,*}, Ali Polat^a, Brian J. Fryer^{a,c}, Yildirim Dilek^d, Mohamed El-Sharkawy^b, Shawki Sakran^b

^a Department of Earth and Environmental Sciences, University of Windsor, Windsor, ON, Canada N9B 3P4

^b Geology Department, Cairo University, Giza 12613, Egypt

^c Great Lake Institute for Environmental Research, University of Windsor, ON, Canada N9B 3P4

^d Department of Geology, Miami University, Oxford, OH 45056, USA

ARTICLE INFO

Article history:

Received 19 May 2009

Received in revised form 6 February 2010

Accepted 22 February 2010

Available online 1 March 2010

Keywords:

Hammamat Group
Retroarc foreland basin
Molasse sediments
Egypt

ABSTRACT

We present new petrographic, and major and trace element data for the Um Hassa Greywacke Member, the uppermost unit of the Hammamat Group, at Wadi Hammamat area, the Eastern Desert of Egypt. The Neoproterozoic Hammamat sedimentary rocks are immature molasse-type rocks that were deposited at the end of the Pan-African Orogeny. The Um Hassa Greywacke Member is bedded, weakly deformed and lies conformably on the polymictic conglomerate of the Um Had Member. The Um Hassa greywackes are poorly sorted and composed mainly of quartz, lithic fragments, and feldspar grains, with an average modal composition of QFL = 53:17:30. Quartz is mostly monocrystalline, feldspars are mainly plagioclase, and lithic fragments are predominantly intermediate to felsic volcanic rocks. The Um Hassa greywackes are characterized by low chemical index of alteration (46–65) and $\text{SiO}_2/\text{Al}_2\text{O}_3$ (4.6–6.1) that indicate limited chemical weathering of the source rocks and deposition close to the source area.

Both point-counting modal analyses and geochemical data suggest that the Um Hassa greywackes were derived from mixed sources. In terms of provenance, continental arc volcanic rocks and oceanic island arc-ophiolitic sources are the main contributors to the sediments of the Um Hassa greywackes. These rock types are exposed in the Eastern Desert as Dokhan-type continental arc volcanic rocks and accreted oceanic arc-ophiolitic mélange, respectively. Considering the geodynamic evolution of the Central Eastern Desert, the Um Hassa greywackes in the Wadi Hammamat area appear to have been deposited in a retroarc foreland basin behind the Dokhan continental arc developed over a west-dipping subduction zone.

© 2010 Elsevier Ltd. All rights reserved.

1. Introduction

The geochemical characteristics of siliciclastic sedimentary rocks are controlled mainly by source composition, weathering, transportation and diagenetic processes (McLennan et al., 1993). Petrography of sandstones has been widely used to discriminate the tectonic setting of provenance (Dickinson and Suczek, 1979; Dickinson et al., 1983; Dickinson, 1985; Hendrix, 2000). The use of geochemical compositions of clastic sedimentary rocks is an important tool for understanding the nature of source rocks (Roser and Korsch, 1988, 1999; McLennan et al., 1993), weathering and erosion dynamics (Nesbitt and Young, 1982, 1996), the tectonic setting of the depositional basins (Bhatia, 1983; Bhatia and Crook, 1986; Roser and Korsch, 1986), and post-depositional changes (Fedò et al., 1995, 1997).

The Eastern Desert of Egypt constitutes the northwestern end of the Nubian segment of the Arabian–Nubian Shield (ANS). The ANS formed through a series of subduction, accretion and crustal thickening processes during the Neoproterozoic Pan-African Orogeny (Engel et al., 1980; Stern, 1994; Johnson and Woldehaimanot, 2003; Abd El-Rahman et al., 2009a,b). Late stages of the crustal evolution of the Eastern Desert are marked by the deposition of the molasse-type Hammamat Group (Eliwa et al., 2006). There are some controversies on the stratigraphic position, grade of metamorphism, structure and tectonic significance of the Hammamat Group (Wilde and Youssef, 2002, and references therein).

The sedimentary rocks of the Hammamat Group are immature clastic rocks that were deposited through fluvial processes (Grothaus et al., 1979; Shalaby et al., 2006). The tectonic setting of such deposits is a matter of debate. Following the intramontane basin hypothesis, Fritz and Messner (1999, and references therein) divided the molasse basins in the Eastern Desert into external foreland basins and Najd strike-slip fault-related extensional

* Corresponding author.

E-mail address: yasser@uwindsor.ca (Y. Abd El-Rahman).

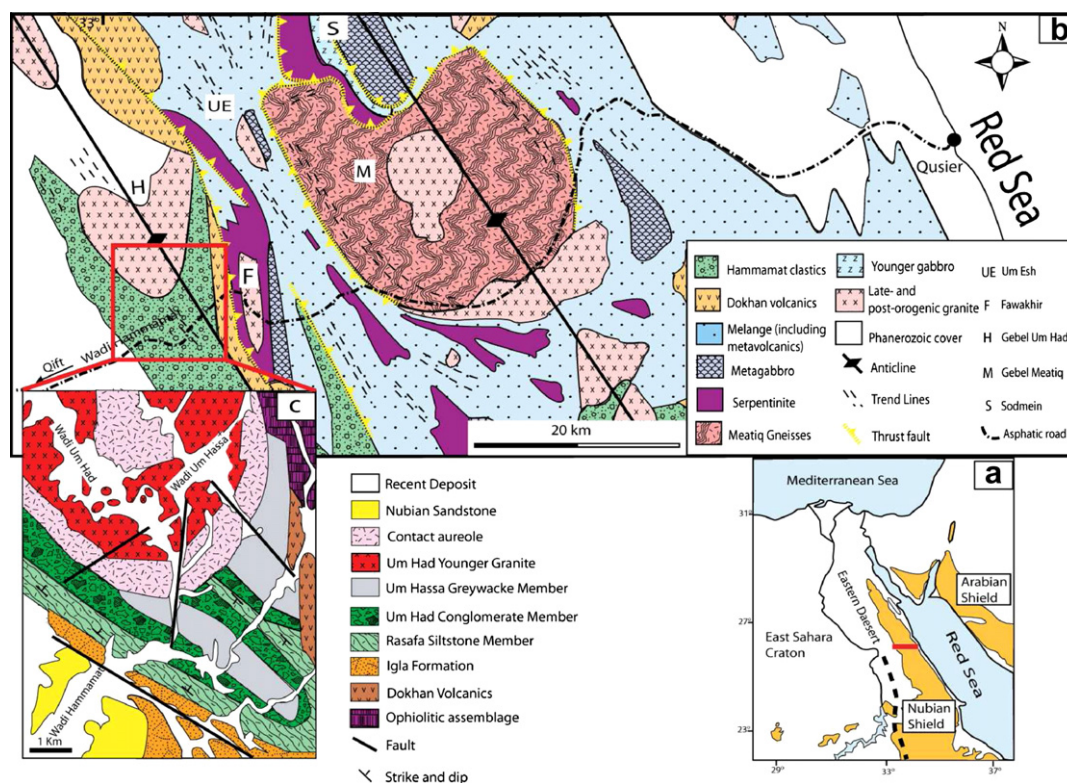


Fig. 1. (a) A generalized map of the Arabian–Nubian Shield rocks (orange) along the Red Sea. The dashed line is the approximate boundary between the Shield and the Eastern Saharan Craton (after Greiling et al., 1994) (red strip represents the area in b). (b) Simplified geological map of the Hammamat–Meatiq region (after El Gaby et al., 1984). (c) Geological map of the Hammamat area (after Holail and Moghazi, 1998). (For interpretation of the references to colour in this figure legend, the reader is referred to the web version of this article.)

basins. Holail and Moghazi (1998) suggested that the Hammamat sediments were deposited in intra-arc basins. Andresen et al. (2009) proposed that they were deposited as piggy-back basins in the Wadi Hammamat area. However, Wilde and Youssef (2001, 2002) argued for the deposition of the Hammamat sediments in a major fluvial system of continental scale rather than deposition in isolated intramontane basins. Their argument based on observing detrital zircons with ages older than Neoproterozoic in the Hammamat sedimentary rocks which suggests derivation of sediments from distal source areas. Ries et al. (1983) suggested that at least the upper part of the Hammamat Group may have been laterally continuous along the Central Eastern Desert.

The Hammamat Group in the Central Eastern Desert was divided into the lower Iqla Formation and the upper Shihimiya Formation (Akaad and Noweir, 1969, 1980). They divided the Shihimiya Formation lithostratigraphically into a lower Rasafa Siltstone Member followed by the Um Had Conglomerate Member and the upper Um Hassa Greywacke Member. This study focuses on the petrographical and geochemical characteristics of the uppermost part of the Hammamat Group, the Um Hassa Greywacke Member in the type locality in the Wadi Hammamat area of the Eastern Desert of Egypt (Fig. 1). The objective of the study is to assess the composition and nature of the source rocks petrographically and geochemically, and to determine the tectonic setting of the Um Hassa Greywacke Member.

2. Field relations and characteristics

The best exposures of the Hammamat Group are located in the west of Qift–Qusier Road at their type locality in the Wadi Hammamat area (Fig. 1b). The thickness of the Hammamat Group at its

type locality reaches up to 4000 m where the most complete succession of this group is preserved (Akaad and Noweir, 1969, 1980). To the west of Wadi Hammamat, the Hammamat Group is unconformably overlain by the Phanerozoic Nubian Sandstone (Fig. 2a) and is juxtaposed to the ophiolitic and arc-related rocks to the east. Towards the north of Qift–Qusier Road, the Hammamat Group is intruded by the Um Had granitic pluton and underwent contact metamorphism (Abu El Ela and El Bahariya, 1995; El Kalio-ubi, 1996; Fowler and Osman, 2001). The emplacement age of the Um Had granites is 596 Ma (Andresen et al., 2009) suggesting that the Hammamat Group was deposited before this time. Ries and Darbyshire (in Ries et al., 1983) suggested that the age of the Hammamat Group should not be older than 616 Ma, which is the age of emplacement of calc-alkaline volcanic rocks (Dokhan Volcanics) that provided pebbles to the Hammamat Group. Although the Dokhan-type volcanic rocks are thrust westwards over the Hammamat sedimentary rocks in the Wadi Hammamat area, the Hammamat sedimentary rocks originally rested unconformably on the Dokhan Volcanics and older units (Akaad and Noweir, 1980).

The Um Hassa Greywacke Member is the uppermost unit of the Hammamat Group and it lies conformably on the Um Had Conglomerate Member (Fig. 1c). Conglomerates of the Um Had Member are massive, poorly sorted and either clast- or matrix-supported. The fragments of the Um Had conglomerate are mostly rounded to sub-angular (Fig. 2b). The conglomerates are polymictic and contain mainly pebbles of the Dokhan-type volcanic rocks, granitic rocks, green tuffs, chert, jasper, and epidosite (Ries et al., 1983). The overlying Um Hassa greywackes are mainly greenish-grey to brown, poorly sorted and bedded. Lamination, graded bedding, and cross bedding are the dominant sedimentary structures. The entire Hammamat Group was folded into open NW–SE trending SW-verging folds (Ries et al., 1983; Holail and Moghazi,

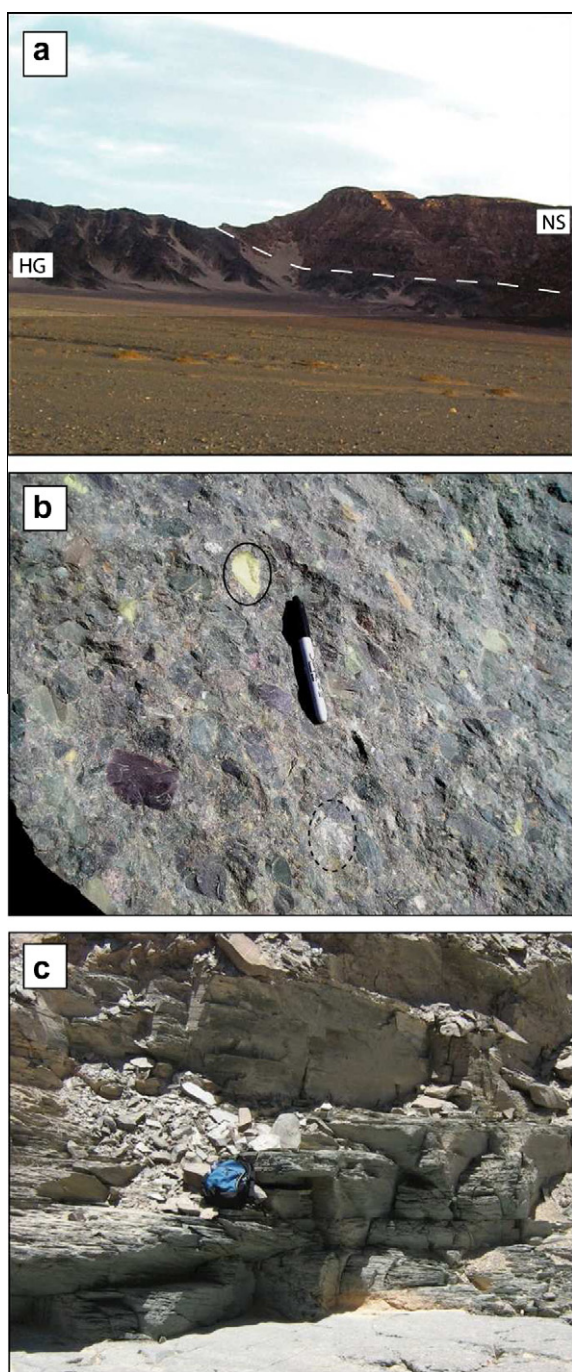


Fig. 2. (a) Precambrian Hammamat Group (HG) is unconformably overlain by Phanerozoic Nubian Sandstone (NS); contact between the two units is along the white dashed lines. (b) Polymictic conglomerate of the Um Had Member. Note the Dokhan-type volcanic rocks in purple, epidosite (solid ellipse) and plagiogranite (dashed ellipse) fragments. (c) Bedded (upper) and cleaved (lower) greywacke of the Um Hassa Member. (For interpretation of the references to colour in this figure legend, the reader is referred to the web version of this article.)

1998; Fowler and El Kalioubi, 2004; Abd El-Wahed, 2007). Pressure-solution cleavage is recorded in the Um Hassa greywackes especially in the fine-grained varieties (Fig. 2c).

3. Petrography

In order to determine the modal composition of the Um Hassa greywackes, eleven medium- to coarse-grained (0.2–1 mm)

samples were counted to about 300 points and the definition for different grain types is adopted from Dickinson (1985). The detrital grains of the Um Hassa greywackes are categorized as monocrystalline quartz (Qm), polycrystalline quartz (Qp), total feldspar (F), plagioclase (P) and K-feldspar (K), and matrix (M) (Table 1). The unstable lithic fragments consist of volcanic/metavolcanic rocks (Lv) and fragments of sedimentary/metasedimentary rocks (Ls). However, total lithic fragments (Lt) stands for unstable lithic fragments and polycrystalline quartz (Lv + Ls + Qp).

The Um Hassa greywackes are poorly to moderately sorted. The detrital grains vary from angular to sub-rounded and are embedded in a mostly silty matrix (>15%). The matrix probably formed from the breaking down of lithic fragments. Quartz is the most abundant detrital component (Fig. 3a). Monocrystalline quartz (average of 23%) is more abundant than polycrystalline quartz (average of 11%). Most quartz grains exhibit undulatory extinction.

Lithic fragments make up 24% of the greywackes. The ratios of the volcanic and sedimentary lithic fragments are variable. Some of the lithic fragments have greenschist facies mineral assemblages. The volcanic lithic fragments are mainly (meta-) andesites and felsites and less abundant mafic volcanic rocks (Fig. 3a). They are characterized by the presence of feldspar laths which are associated with quartz, sericite, chlorite, and/or epidote. The coarse-grained greywackes contain some microgranitic fragments with micrographic and myrmekitic quartz-feldspar intergrowths. The sedimentary lithic fragments comprise phyllosilicate-rich rocks such as quartz-sericite rocks (Fig. 3b). Sericite–chlorite and quartz-sericite schist fragments are classified as sedimentary lithic fragments.

Feldspar fragments constitute about 11% of the Um Hassa greywackes. Plagioclase (10%) is far more abundant than K-feldspar (1%). Plagioclase fragments are mostly fresh showing albite twinning (Fig. 3c). However, altered, mainly sericitized, plagioclase grains are not uncommon. Other detrital components of the Um Hassa greywackes are epidote, mica, opaque minerals, chlorite, and carbonates (calcite) in order of decreasing abundance. Epidote, opaque minerals, and carbonates are represented by dispersed equant grains (Fig. 3d). On the other hand, micas are represented by long, commonly bent, muscovite flakes (Fig. 3b). The matrix of the Um Hassa greywackes consists mainly of silt-size quartz, feldspar, chlorite, and epidote. Holail and Moghazi (1998) reported the presence of illite. Epidote and calcite occur, to a limited extent, as authigenic crystalline patches within the matrix.

4. Analytical methods

About 300–500 g chips of the Um Hassa greywackes (0.2–1 mm) were crushed and pulverized using an agate mill in the Department of Earth and Environmental Sciences, University of Windsor, Canada. Major elements and Sc were analyzed by a Thermo Jarrell-Ash Enviro II ICP at ACTLABS in Ancaster, Canada. The samples were fused then dissolved in 5% nitric acid. Totals of major element oxides are 100 ± 1 wt.% and the analytical precisions are 1–2%. International standards, DNC-1 and BIR-1, were used to estimate the accuracy of the major elements (Table 2).

Samples were analyzed for rare earth elements (REE), high field strength elements (HFSE), large ion lithophile elements (LILE) and transition metals (Ni, Co, Cr and V) by a high-sensitivity Thermo Elemental X7 ICP-MS in the Great Lakes Institute for Environmental Research (GLIER), University of Windsor, Canada, using the protocol of Jenner et al. (1990). Samples were dissolved in a concentrated HF-HNO₃ mixture in screw-top Teflon (Saville[®]) bombs and further attacked by HNO₃–H₃BO₃–H₂C₂O₄ and then with 50% HNO₃. Analytical precisions are estimated as follows: 1–10% for REE, Rb, Sr, Ba, Y, Nb, Co, Cu, Zr, and U; 10–20% for V,

Table 1
Modal composition of Um Hassa greywackes.

| | Q | F | L | Qm | Qp | P | K | Lv | Ls | Lt | Misc | M |
|----------|------|------|------|------|------|------|-----|------|------|------|------|------|
| EGY04-24 | 41.6 | 10.3 | 16.4 | 29.4 | 12.2 | 8.2 | 2.1 | 12.2 | 4.2 | 28.6 | 12 | 19.7 |
| EGY04-25 | 41.3 | 10.2 | 15.2 | 26.3 | 15 | 8 | 2.2 | 10.2 | 5 | 30.2 | 10.6 | 22.7 |
| EGY04-26 | 34.3 | 8 | 18.5 | 25.7 | 8.6 | 7.5 | 0.5 | 11.8 | 6.7 | 27.1 | 15.2 | 24 |
| EGY04-27 | 41 | 15.3 | 12 | 27.1 | 13.9 | 13.4 | 1.9 | 8.7 | 3.3 | 25.9 | 9.3 | 22.4 |
| EGY04-28 | 35.6 | 13 | 19.6 | 21.5 | 14.1 | 12.9 | 0.1 | 14.1 | 5.5 | 33.7 | 7.9 | 23.9 |
| EGY04-29 | 32 | 12.3 | 13 | 24.1 | 7.9 | 12.3 | 0 | 10.9 | 2.1 | 20.9 | 17.3 | 25.4 |
| EGY04-30 | 29.2 | 10 | 23.7 | 20.8 | 8.4 | 8.9 | 1.1 | 15 | 8.7 | 32.1 | 11.8 | 25.3 |
| EGY04-31 | 24 | 11.4 | 25.1 | 16 | 8 | 9.5 | 1.9 | 11.9 | 13.2 | 33.1 | 14.4 | 25.1 |
| EGY04-32 | 28.2 | 9.6 | 23.4 | 19.8 | 8.4 | 8.7 | 0.9 | 16.5 | 6.9 | 31.8 | 10.2 | 28.6 |
| EGY06-03 | 27.3 | 9.1 | 27 | 18.2 | 9.1 | 8.4 | 0.7 | 17.2 | 9.8 | 36.1 | 9.1 | 27.5 |
| EGY06-05 | 37.3 | 6.8 | 16.3 | 26.6 | 10.7 | 6.8 | 0 | 14.5 | 1.8 | 27 | 15.1 | 24.5 |
| Average | 34 | 11 | 19 | 23 | 11 | 10 | 1 | 13 | 6 | 30 | 12 | 24 |

Qm: Monocrystalline quartz; Qp: polycrystalline quartz; Q: total quartz (Qm + Qp); P: plagioclase; K: potassium feldspar; F: total feldspar (P + K); Lv: volcanic and meta-volcanic lithic fragments; Ls: sedimentary and metasedimentary lithic fragments; L: lithic fragments (Lv + Ls); Lt: total lithic fragments (Lv + Ls + Qp), Misc: other grains (epidote, mica, iron oxides, carbonates); M: matrix.

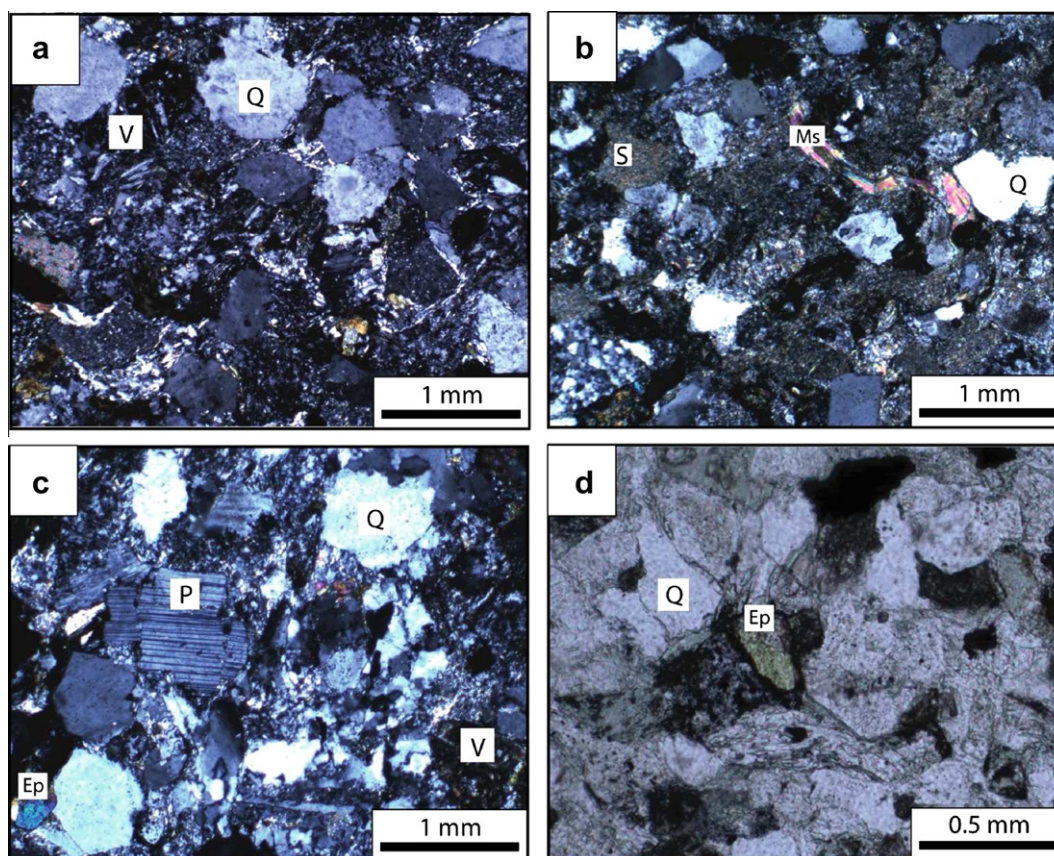


Fig. 3. Photomicrographs of Um Hassa greywackes showing different kinds of framework components: (a) monocrystalline quartz (Q) and volcanic fragments (V), (b) sedimentary fragments (S) and bent muscovite (Ms), (c) fractured plagioclase with albite twinning (P), and (d) epidote (Ep) and opaque grains.

Ni, Zn, Cs, Mo, and Ga; and 20–30% for Ta, Th, Cr, and Pb. BHVO-1 and BHVO-2, were used as international reference materials to estimate accuracy of the measured trace elements (Table 3).

5. Geochemical results

Major and trace element compositions of the Um Hassa greywackes are given in Table 4. The Um Hassa samples plot mostly in the greywacke field of the log (SiO₂/Al₂O₃) versus log (Na₂O/K₂O) classification diagram of Pettijohn et al. (1972) (Fig. 4). In terms of major elements, the Um Hassa greywackes are character-

ized by 64.2–70.4 wt.% SiO₂, 1.9–2.8 wt.% MgO, and 4.2–6.5 wt.% Fe₂O₃. The MgO and Fe₂O₃ (Fig. 5a and b), as well as TiO₂, are negatively correlated with SiO₂. The concentrations of MgO and Fe₂O₃ are higher than the average upper continental crust (UCC: Fig. 5) values of Taylor and McLennan (1985). On the other hand, Al₂O₃ (11.2–14.58 wt.%) and K₂O (1.32–2.41 wt.%) of the Um Hassa greywackes do not show any significant correlation with SiO₂ and their values are lower than those of UCC (Fig. 5c and d).

The Um Hassa greywackes have LREE-enriched chondrite-normalized patterns similar to Post-Archean Australian Shale (PAAS) and UCC patterns (Fig. 6a). However, the Um Hassa greywacke patterns are slightly less fractionated (La/Sm_n = 2.4–3.3) relative to

Table 2

Measured and recommended major elements values for DNC-1 (recommended by USGS) and BIR-1 (recommended by Max-Planck-Institute) standards.

| Element | DNC-1 | | BIR-1 | |
|---|----------|-------------|----------|-------------|
| | Measured | Recommended | Measured | Recommended |
| SiO ₂ (wt.%) | 48.1 | 47.2 | 49.0 | 47.7 |
| Al ₂ O ₃ | 18.7 | 18.3 | 15.8 | 15.4 |
| Fe ₂ O ₃ ^(T) | 9.76 | 9.97 | 11.26 | 11.3 |
| MnO | 0.15 | 0.15 | 0.18 | 0.18 |
| MgO | 10.2 | 10.1 | 9.68 | 9.68 |
| CaO | 11.6 | 11.3 | 13.7 | 13.4 |
| Na ₂ O | 1.67 | 1.89 | 1.6 | 1.81 |
| K ₂ O | 0.27 | 0.23 | 0.09 | 0.03 |
| TiO ₂ | 0.49 | 0.48 | 0.99 | 0.97 |
| P ₂ O ₅ | 0.08 | 0.07 | 0.03 | 0.027 |

Table 3

Measured and recommended values for USGS standards BHVO-1 and BHVO-2 (recommended by Max-Planck-Institute).

| Element | BHVO-2 (n = 21) | | BHVO-1 (n = 11) | |
|----------|-----------------|-------------|-----------------|-------------|
| | Measured | Recommended | Measured | Recommended |
| Li (ppm) | 4.2 | 4.6 | 4.69 | 4.6 |
| V | 313 | 317 | 321 | 318 |
| Cr | 258 | 280 | 247 | 287 |
| Co | 44 | 45 | 45 | 45 |
| Ni | 155 | 119 | 150 | 118 |
| Cu | 133 | 127 | 144 | 137 |
| Zn | 110 | 103 | | |
| Rb | 8.9 | 9.11 | 9.2 | 9.19 |
| Sr | 382 | 396 | 390 | 396 |
| Y | 22.8 | 26.0 | 23.3 | 26 |
| Zr | 156 | 172 | 165 | 174 |
| Nb | 14.3 | 18.1 | 14.9 | 18.6 |
| Cs | 0.10 | 0.1 | 0.11 | 0.13 |
| Ba | 128 | 131 | 128 | 133 |
| La | 14.7 | 15.2 | 14.8 | 15.5 |
| Ce | 36.7 | 37.5 | 37.0 | 38.1 |
| Pr | 5.18 | 5.35 | 5.13 | 5.42 |
| Nd | 23.8 | 24.5 | 23.4 | 24.7 |
| Sm | 5.90 | 6.07 | 5.83 | 6.112 |
| Eu | 1.98 | 2.07 | 1.97 | 2.09 |
| Gd | 6.23 | 6.24 | 6.20 | 6.33 |
| Tb | 0.89 | 0.92 | 0.91 | 0.96 |
| Dy | 5.1 | 5.31 | 5.10 | 5.13 |
| Ho | 0.94 | 0.98 | 0.95 | 0.98 |
| Er | 2.5 | 2.54 | 2.47 | 2.55 |
| Tm | 0.32 | 0.33 | 0.31 | 0.33 |
| Yb | 1.92 | 2.00 | 1.88 | 2 |
| Lu | 0.26 | 0.28 | 0.26 | 0.27 |
| Hf | 4.23 | 4.36 | 4.52 | 4.46 |
| Ta | 0.9 | 1.14 | 0.86 | 1.21 |
| Pb | 2.58 | 1.6 | 4.18 | 2.4 |
| Th | 1.6 | 1.20 | 1.40 | 1.23 |
| U | 0.43 | 0.403 | 0.44 | 0.409 |

UCC (La/Sm_n = 4.3). Europium anomalies in the greywackes (Eu/Eu* = 0.61–0.79) are similar to that of UCC (Eu/Eu* = 0.65). Upper continental crust-normalized patterns for the Um Hassa greywackes reveal significant enrichment of Cr (234–434 ppm) and Ni (49–72 ppm) but depletions in Nb (4.1–7.7 ppm), Rb (33–63 ppm), and Th (3.64–8.92 ppm) relative to UCC values (35, 20, 25, 112 and 10.7 ppm, respectively) (Fig. 6b).

6. Discussion

6.1. Effects of sedimentary processes on geochemistry

Although the geochemistry of siliciclastic sedimentary rocks can be used to study their provenance, the reliability of the geochemical composition as a provenance indicator can be altered

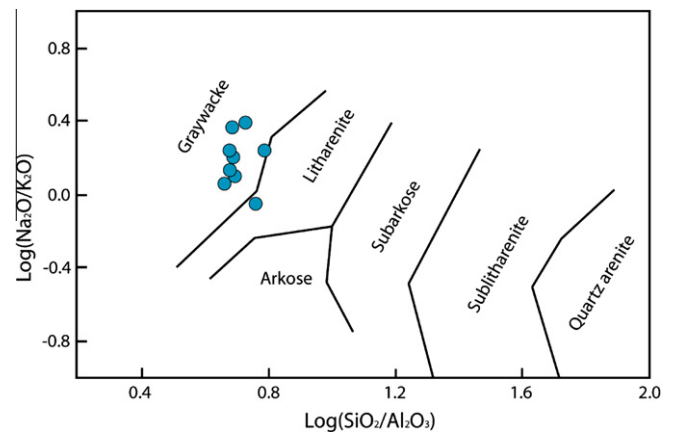


Fig. 4. Log (Na₂O/K₂O) versus Log (SiO₂/Al₂O₃) of Pettijohn et al. (1972) for chemical classification of sandstones.

by weathering, transportation, and diagenesis processes. The effects of such processes on major and trace element geochemistry of siliciclastic sediments are variable. Chemical weathering is considered a major contributor to compositional changes of siliciclastic sediments (Nesbitt, 2003).

Given that the Hammamt group of Wadi Hammamt was derived mostly from igneous sources (Holail and Moghazi, 1998), the effect of weathering can be assessed using the chemical index of alteration (CIA = [Al₂O₃/(Al₂O₃ + CaO* + Na₂O + K₂O)] * 100) of Nesbitt and Young (1982). The CIA values of the Um Hassa greywackes are low (48–65). These values are closer to the unweathered upper crust CIA value (50), than to the average shale CIA values (70–75) of Taylor and McLennan (1985), which indicates limited chemical weathering of the source rocks. On the Al₂O₃–(CaO* + Na₂O)–K₂O diagram (Fig. 7a), the Um Hassa greywackes cluster on the left side of the K-feldspar-plagioclase tie line with slight excursion towards the Al₂O₃ apex which confirms the weakly weathered nature of the source rocks (Nesbitt and Young, 1984; Holail and Moghazi, 1998).

Erosion and transport of weathered rocks may create chemical differentiation, but not chemical changes, of the transported sediments through hydraulic sorting (Nesbitt and Young, 1996). The Um Hassa greywackes show high angularity of the fragments and poor sorting which suggest high erosion rates of the source rock and rapid sedimentation (Camirè et al., 1993; Nesbitt, 2003). This refutes the possibility of long transportation and sorting that may cause chemical differentiation through clay separation. Due to an increase of quartz at the expense of clay during sediment transport and recycling, the SiO₂/Al₂O₃ ratio can be used to measure the degree of sediment maturity (Roser and Korsch, 1999). The average value of SiO₂/Al₂O₃ ratio for the Um Hassa greywacke is about 5, which is considered by Zhang (2004) to be low indicating immature sediments deposited close to their source.

Diagenetic processes may cause significant changes in the chemical composition of the clastic sedimentary rocks; however, it is possible to use the geochemical data to address the provenance of clastic sedimentary rocks (McLennan et al., 2003). Mechanical compaction rather than chemical compaction is noticed in the Um Hassa greywackes. Chemical compaction refers to the compaction processes involving dissolution and precipitation of minerals (Middleton, 2003). Mechanical compaction of the Umm Hassa greywackes resulted in squeezing of sericite- and chlorite-rich fragments against competent fragments, bending of muscovite flakes, and fracturing of feldspar grains (Fig. 3b and c). Formation of the matrix might have been resulted from the disintegration of labile grains (c.f. Whetten and Hawkins, 1970) but the

Table 4
Chemical composition of Um Hassa greywackes.

| | EGY-04-24 | EGY-04-25 | EGY-04-26 | EGY-04-27 | EGY-04-28 | EGY-04-29 | EGY-04-30 | EGY-04-31 | EGY-04-32 |
|--|-----------|-----------|-----------|-----------|-----------|-----------|-----------|-----------|-----------|
| SiO ₂ (wt.%) | 68.8 | 70.4 | 65.9 | 68.0 | 69.9 | 64.2 | 67.1 | 66.9 | 66.2 |
| Al ₂ O ₃ | 11.2 | 12.3 | 14.5 | 14.0 | 13.3 | 13.1 | 13.8 | 13.9 | 13.9 |
| Fe ₂ O ₃ | 5.66 | 4.18 | 6.48 | 5.36 | 4.84 | 6.35 | 5.44 | 5.68 | 6.01 |
| MnO | 0.13 | 0.10 | 0.14 | 0.19 | 0.13 | 0.17 | 0.14 | 0.09 | 0.09 |
| MgO | 1.92 | 2.1 | 2.77 | 2.48 | 2.15 | 2.42 | 2.45 | 2.36 | 2.51 |
| CaO | 4.03 | 2.2 | 1.42 | 1.4 | 1.59 | 2.95 | 2.16 | 2.15 | 2.81 |
| Na ₂ O | 2.33 | 2.16 | 2.22 | 3.5 | 3.59 | 2.67 | 3.08 | 2.96 | 2.87 |
| K ₂ O | 1.32 | 2.41 | 1.93 | 1.51 | 1.45 | 2.11 | 1.91 | 2.2 | 1.66 |
| TiO ₂ | 0.96 | 0.53 | 0.97 | 0.60 | 0.59 | 0.92 | 0.67 | 0.73 | 0.86 |
| P ₂ O ₅ | 0.17 | 0.14 | 0.24 | 0.15 | 0.15 | 0.21 | 0.18 | 0.19 | 0.22 |
| LOI | 2.75 | 2.72 | 3.66 | 3.33 | 3.37 | 3.43 | 3.19 | 2.9 | 3.05 |
| Total | 99.22 | 99.15 | 100.2 | 100.6 | 101 | 98.58 | 100.1 | 100.1 | 100.2 |
| Sc (ppm) | 14 | 11 | 17 | 13 | 12 | 15 | 13 | 14 | 15 |
| Zr | 161 | 128 | 257 | 122 | 139 | 260 | 123 | 164 | 227 |
| V | 138 | 76 | 141 | 101 | 93 | 127 | 100 | 117 | 123 |
| Li | 12.5 | 13.6 | 28.3 | 24.2 | 21.7 | 21.7 | 21.3 | 23.4 | 20.0 |
| V | 227 | 163 | 199 | 183 | 140 | 222 | 138 | 184 | 148 |
| Cr | 434 | 335 | 338 | 339 | 247 | 401 | 242 | 301 | 234 |
| Co | 13 | 12 | 13 | 15 | 12 | 17 | 10 | 15 | 15 |
| Ni | 66 | 54 | 84 | 59 | 49 | 72 | 71 | 58 | 69 |
| Cu | 49 | 22 | 46 | 41 | 40 | 43 | 44 | 39 | 41 |
| Zn | 95 | 114 | 135 | 101 | 98 | 518 | 165 | 248 | 125 |
| Ga | 49 | 65 | 59 | 69 | 62 | 69 | 67 | 70 | 65 |
| Rb | 33 | 60 | 57 | 45 | 39 | 63 | 55 | 61 | 50 |
| Sr | 432 | 240 | 134 | 227 | 228 | 280 | 287 | 273 | 552 |
| Y | 27.3 | 21.9 | 32.4 | 21.7 | 21.7 | 29.2 | 22.8 | 24.6 | 29.0 |
| Nb | 6.53 | 4.10 | 7.70 | 4.96 | 4.75 | 6.57 | 5.03 | 6.04 | 6.73 |
| Mo | 0.84 | 0.70 | 0.81 | 0.57 | 0.72 | 0.96 | 0.72 | 0.61 | 0.55 |
| Cs | 1.15 | 2.34 | 2.07 | 1.48 | 1.23 | 2.48 | 1.50 | 1.60 | 1.42 |
| Ba | 301 | 498 | 330 | 514 | 458 | 535 | 526 | 548 | 453 |
| La | 33.2 | 14.4 | 30.6 | 16.8 | 19.5 | 26.8 | 18.8 | 22.3 | 27.3 |
| Ce | 73.9 | 36.4 | 65.5 | 39.9 | 45.5 | 58.0 | 43.3 | 47.9 | 60.8 |
| Pr | 8.50 | 4.17 | 8.10 | 4.57 | 5.16 | 7.29 | 5.21 | 5.94 | 7.28 |
| Nd | 32.4 | 17.2 | 33.0 | 19.0 | 21.4 | 28.3 | 21.2 | 23.7 | 29.2 |
| Sm | 6.43 | 3.83 | 6.95 | 4.48 | 4.63 | 5.91 | 4.45 | 5.21 | 5.88 |
| Eu | 1.24 | 1.03 | 1.47 | 1.02 | 1.14 | 1.33 | 1.14 | 1.23 | 1.35 |
| Gd | 6.00 | 4.17 | 6.59 | 4.36 | 4.71 | 6.08 | 4.82 | 5.10 | 6.07 |
| Tb | 0.84 | 0.63 | 1.01 | 0.67 | 0.69 | 0.91 | 0.70 | 0.74 | 0.93 |
| Dy | 5.03 | 3.91 | 5.92 | 3.85 | 4.05 | 5.48 | 4.42 | 4.52 | 5.47 |
| Ho | 1.03 | 0.80 | 1.24 | 0.82 | 0.80 | 1.14 | 0.84 | 0.92 | 1.09 |
| Er | 3.07 | 2.54 | 3.64 | 2.47 | 2.41 | 3.26 | 2.57 | 2.74 | 3.26 |
| Tm | 0.46 | 0.36 | 0.53 | 0.35 | 0.37 | 0.48 | 0.38 | 0.40 | 0.48 |
| Yb | 2.89 | 2.32 | 3.36 | 2.38 | 2.31 | 3.07 | 2.36 | 2.49 | 3.10 |
| Lu | 0.43 | 2.07 | 0.52 | 0.36 | 0.35 | 0.49 | 0.37 | 0.38 | 0.56 |
| Ta | 0.59 | 0.36 | 0.71 | 0.42 | 0.42 | 0.59 | 0.44 | 0.53 | 0.61 |
| Pb | 20 | 44 | 40 | 28 | 49 | 22 | 118 | 25 | 29 |
| Bi | 0.19 | 0.20 | 0.18 | 0.25 | 0.22 | 0.29 | 0.21 | 0.28 | 0.25 |
| Th | 7.14 | 3.64 | 8.92 | 4.47 | 4.84 | 8.63 | 4.53 | 5.91 | 7.64 |
| U | 2.52 | 1.59 | 2.94 | 1.65 | 1.66 | 3.73 | 1.97 | 2.27 | 2.98 |
| SiO ₂ /Al ₂ O ₃ | 6.1 | 5.7 | 4.6 | 4.8 | 5.3 | 4.9 | 4.9 | 4.8 | 4.8 |
| CIA | 48 | 56 | 65 | 59 | 57 | 53 | 56 | 57 | 56 |
| Eu/Eu* | 0.61 | 0.79 | 0.67 | 0.71 | 0.75 | 0.68 | 0.76 | 0.73 | 0.69 |
| La/Yb _{cn} | 8.2 | 4.5 | 6.5 | 5.1 | 6.1 | 6.3 | 5.7 | 6.4 | 6.3 |
| Gd/Yb _{cn} | 1.71 | 1.48 | 1.62 | 1.51 | 1.69 | 1.64 | 1.68 | 1.69 | 1.62 |
| La/Sm _{cn} | 3.3 | 2.4 | 2.8 | 2.4 | 2.7 | 2.9 | 2.7 | 2.8 | 3.0 |
| Th/Sc | 0.51 | 0.33 | 0.52 | 0.34 | 0.40 | 0.58 | 0.35 | 0.42 | 0.51 |
| Th/U | 2.8 | 2.3 | 3.0 | 2.7 | 2.9 | 2.3 | 2.3 | 2.6 | 2.6 |

pseudo-matrix represented by deformed fine-grained lithic grains is also noticeable (c.f. Zhang et al., 2008). Both compaction and matrix formation decreased porosity and thus hindered cementation, which is confirmed microscopically through the absence of cement phases. On the Al₂O₃–(CaO* + Na₂O)–K₂O diagram (Fig. 7a), the samples show small scatter towards the K₂O apex which may suggest minor K-metasomatism (c.f. Nesbitt and Young, 1989). This process can occur through the transformation of aluminous clay in the matrix into illite and/or conversion of plagioclase to K-feldspar (Fedo et al., 1995). As the plagioclase grains of the Um Hassa greywackes are fresh and illite is found in the greywacke sediments of Wadi Hammamat (Holail and Moghazi, 1998), transfor-

mation of aluminous clay minerals into illite is the reason for the limited K-metasomatism. Chlorite also occurs in the matrix. If it was not detrital in origin, chlorite could have formed at the expense of the kaolinite in case of limited availability of K in the system (c.f. Worden and Burley, 2003) or by diagenetic transformation of Fe-rich clays (Aagaard et al., 2000; Grigsby, 2001). Illite and chlorite form during late diagenetic stages (Aagaard and Jahren, 1992) that may indicate limited element mobility into or out of the system. The limited chemical effects of weathering and the sedimentary processes during the formation of the Um Hassa greywackes indicate their reliability in determining the provenance of their sediments.

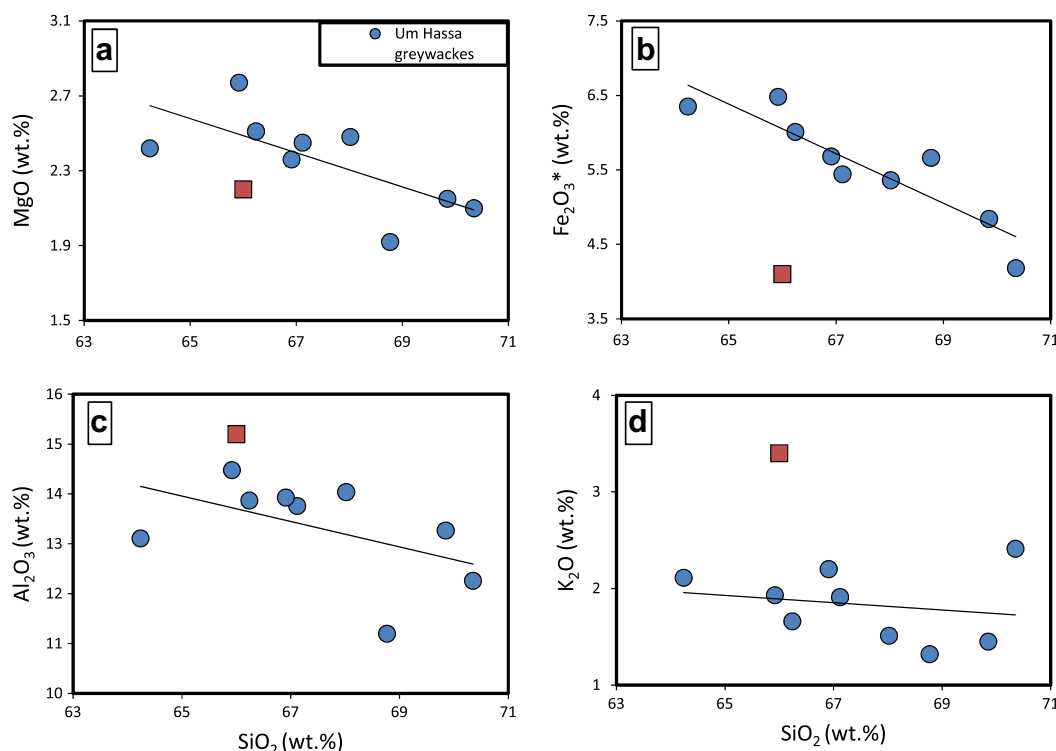


Fig. 5. Variation diagrams of SiO₂ plotted against: (a) MgO, and (b) Fe₂O₃, (c) Al₂O₃, (d) K₂O. Upper Continental Crust (UCC) values are from Taylor and McLennan (1985).

6.2. Provenance

The source region of coarse- and medium-grained clastic sedimentary rocks can be inferred from the types and the relative abundances of their grains. The main lithic fragments in the Um Hassa greywackes are andesite and felsites with some metabasalt and metasedimentary rocks. This mixture indicates multiple sources that could be the Dokhan continental arc volcanic rocks and older intra-oceanic island arc metavolcanics and their associated sedimentary rocks. The same conclusion was reached by Abu El Ela and El Bahariya (1995), El Kalioubi (1996) and Holail and Moghazi (1998) for the Hammamat sedimentary rocks in the Central Eastern Desert and by Osman et al. (2001) for the Northern Eastern Desert. The contribution of both Dokhan Volcanics and the island arc metavolcanics and associated sediments are recorded generally by the whole Hammamat Group (Akaad and Noweir, 1969, 1980). Ries et al. (1983) noticed the same types of fragments in the underlying Um Had Conglomerate Member in addition to granitic rock fragments. In addition to lithic fragments, quartz and plagioclase are also abundant in the Um Hassa greywackes. The presence of quartz and plagioclase grains may reflect a contribution from a granitic source. The undulatory nature of some quartz grains may suggest a metamorphic source (Basu et al., 1975), however it does not exclude the possibility for a plutonic source.

Due to limited weathering of the source rocks (low CIA) and the chemical immaturity of the greywackes (low Al₂O₃/SiO₂), the provenance can be addressed on the basis of the geochemical composition of the sedimentary units. A discrimination diagram proposed by Roser and Korsch (1988) is used to discriminate possible sources (Fig. 7b). The major element compositions of nearby exposed rocks, including the Dokhan Volcanics and felsites of Wadi Sodmein (Asran et al., 2005), the gneissic granitoids of Qift–Qusier Road (Heikal, 2003), and the Fawakhir ophiolites (Abd El-Rahman et al., 2009a) are compared with that of Um Hassa greywackes.

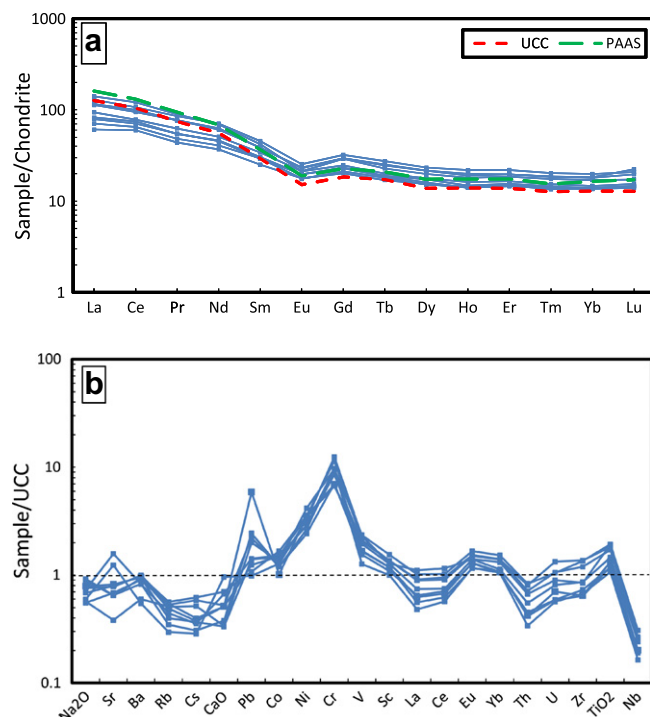


Fig. 6. (a) Chondrite-normalized REE patterns for Um Hassa greywackes. Chondrite values are from Sun and McDonough (1989), UCC and Post-Archean Average Shale (PAAS) values are from Taylor and McLennan (1985). (b) Upper Continental crust-normalized diagram for Um Hassa greywackes. UCC values are from Taylor and McLennan (1985).

The Um Hassa greywackes plot between the Dokhan Volcanics and the gneissic granitoids and the Fawakhir ophiolitic rocks that

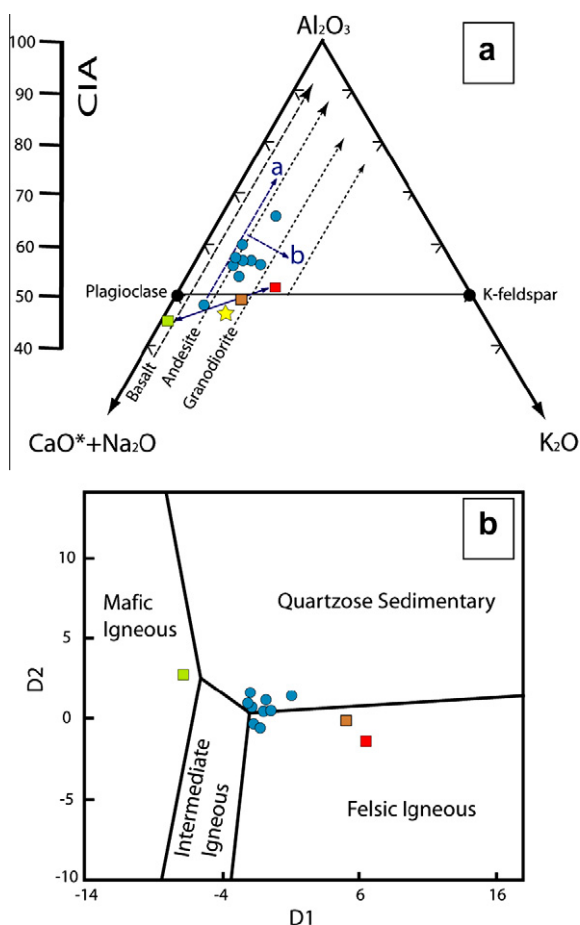


Fig. 7. (a) A-CN-K ternary diagram of molecular proportions of Al_2O_3 –($CaO + Na_2O$)– K_2O for Um Hassa greywackes with chemical index of alteration scale (CIA). Dashed black arrows represent weathering trends of different rocks. Dashed blue arrow (a) represents weathering trends of the greywackes and dashed blue line (b) represents K-metasomatism trend. The blue double headed arrow connects the possible source rocks from the Eastern Desert. Green square is the ophiolitic rocks from Abd El-Rahman et al. (2009a); Brown Square represents Dokhan Volcanics (from Asran et al., 2005); Red square represent Meatiq gneisses (from Heikal, 2003); Yellow star is a plot of UCC from Taylor and McLennan (1985). (Molecular proportions calculations are after Fedo et al. (1995)). (b) Provenance discrimination diagrams according to Roser and Korsch (1988). Symbols as in (a). (For interpretation of the references to colour in this figure legend, the reader is referred to the web version of this article.)

may indicate derivation mainly from these sources. Limited contribution from recycled sedimentary rocks may be indicated from extension of samples to the quartzose sedimentary field. On the CN-A-K diagram (Fig. 7a), the sample with the least weathered fragments (Lowest CIA) lies on the tie line connecting the gneissic granitoids–the Dokhan Volcanics–the ophiolitic rocks, suggesting again the large contribution of the above mentioned rock units to the fragments of the Um Hassa greywackes.

Provenance terranes have been classified depending on the framework modes (Dickinson and Suczek, 1979; Dickinson et al., 1983) and geochemistry of the sedimentary rocks (McLennan et al., 1993). On the Q-F-L diagram (Fig. 8a), the Um Hassa greywackes plot parallel to the quartz-lithic fragments line mainly in the recycled orogen field with an extension towards the arc orogen field. The overlapping area located between the arc orogen and recycled orogen field increases on the Qm-F-L diagram (Fig. 8b). According to Dickinson and Suczek (1979), the recycled orogen field indicates that the sediments were derived from a subduction complex; collisional zone and/or foreland uplift. The contribution

from a subduction complex and arc terranes to the Um Hassa greywackes is recognized through the Qp-Lv-Ls ternary diagram where the samples spread between the subduction complex field and the arc orogen field (Fig. 8c).

From the geochemical perspective, McLennan et al. (1993) classified source rocks into older upper continental crust, recycled sedimentary rocks, younger, differentiated and undifferentiated arc, and exotic terrane-types. The limited input from an older upper continental crust and recycled sedimentary rocks to the Um Hassa greywackes is inferred from low Th/Sc ratios (0.33–0.58) and Zr contents (122–260 ppm). The lower content of Nb relative to UCC indicates an arc source for the Um Hassa greywackes (c.f. Zhang, 2004) which is supported by modal analyses (Fig. 8). In addition to lower Th/Sc ratios, lower LREE ($La/Sm_n = 2.4–3.3$) and Th/U (2.3–3) ratios suggest a significant contribution from arc-derived material (c.f. McLennan et al., 1993). Negative Eu anomalies (Fig. 6a) in the Um Hassa greywackes indicate a contribution from differentiated felsic volcanics and plutonic rocks of a dissected magmatic arc. El-Bouseily (1986) stated that the granitic pebbles from the Um Had Conglomerate Member are mostly low- Al_2O_3 trondhjemite and are similar to some varieties of older granitoids of Egypt. Their chemical characteristics are similar to volcanic arc trondhjemite associated with oceanic island arc-related volcanic rocks in the Central Eastern Desert (Abdel Rahman, 2004). The exposed arc plutonic core could have been the main source of the monocrystalline quartz and plagioclase distributed in the Um Hassa greywackes. The Um Hassa greywackes are characterized by high Cr (234–434 ppm) and Ni (49–72 ppm). The high contents of these elements in sediments indicate a proximal ophiolitic source (Hiscott, 1984; McLennan et al., 1990, 1993; Garver et al., 1996).

6.3. Tectonic setting

In terms of the tectonic setting, there is a close relationship between the tectonic setting of depositional basins and the geochemical characteristics of their sandstones (Bhatia, 1983; Bhatia and Crook, 1986). Quartz proportion (24–42%), SiO_2 content (67–73 wt.%) and K_2O/Na_2O ratio (0.4–1.1) in the Um Hassa greywackes are similar to those in greywackes deposited at an Andean-type continental margin (c.f. Crook, 1974; Schwab, 1975). The same conclusion is reached by using the K_2O/Na_2O versus SiO_2 plot of Roser and Korsch (1986) where the Um Hassa greywackes plot in the active continental margin field (Fig. 9a).

Bhatia (1983) and Bhatia and Crook (1986) inferred the tectonic settings of sandstones by using major and trace element compositions. The applicability of these tectonic discrimination diagrams for the Hammamat Group was criticized by Holail and Moghazi (1998) due to the mixing of mafic and felsic rocks of different tectonic settings. Although our study of the Um Hassa greywackes confirms various sources, the greywackes plot consistently on the same fields of different tectonic discrimination diagrams. Most of the greywackes plot in the continental arc field and extend into the oceanic arc field (Fig. 9b–d).

The tectonic setting of the Um Hassa greywacke Member can be inferred from the context of the geological evolution of the surrounding rocks in the Central Eastern Desert. According to Abd El-Rahman et al. (2009a), rocks of the Central Eastern Desert, exposed along Qift-Qusier Road, developed through the accretion of island arc-ophiolitic rocks to a passive continental margin to the west along an east-dipping subduction zone. Following the accretion, the polarity of subduction reversed and an Andean-type margin established above a west-dipping subduction zone. The Dokhan Volcanics, which are the surface manifestation of the continental arc magmatism (Eliwa et al., 2006), were formed on the accreted island arc-ophiolitic substrate. The molasse-type basins of the

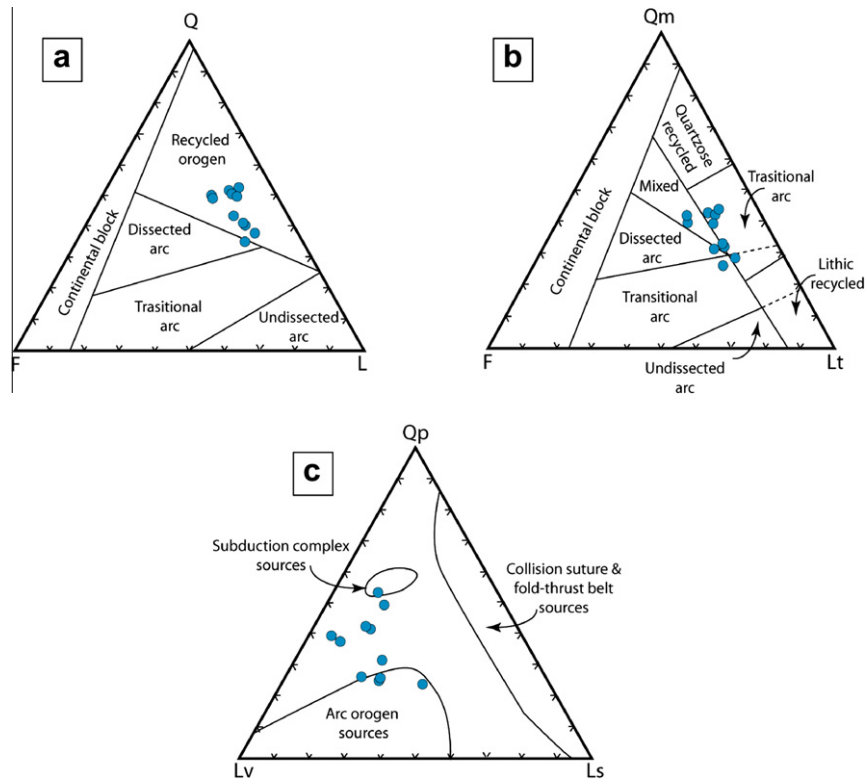


Fig. 8. Modal sandstone ternary plots for Um Hassa greywackes (after Dickinson, 1985): (a) quartz (Q)-feldspar (F)-lithic fragments (L), (b) monocrystalline quartz (Qm)-feldspar (F)-total lithic fragments (Lt), and (c) polycrystalline quartz (Qp)-volcanic lithic fragments (Lv)-sedimentary lithic fragments (Ls).

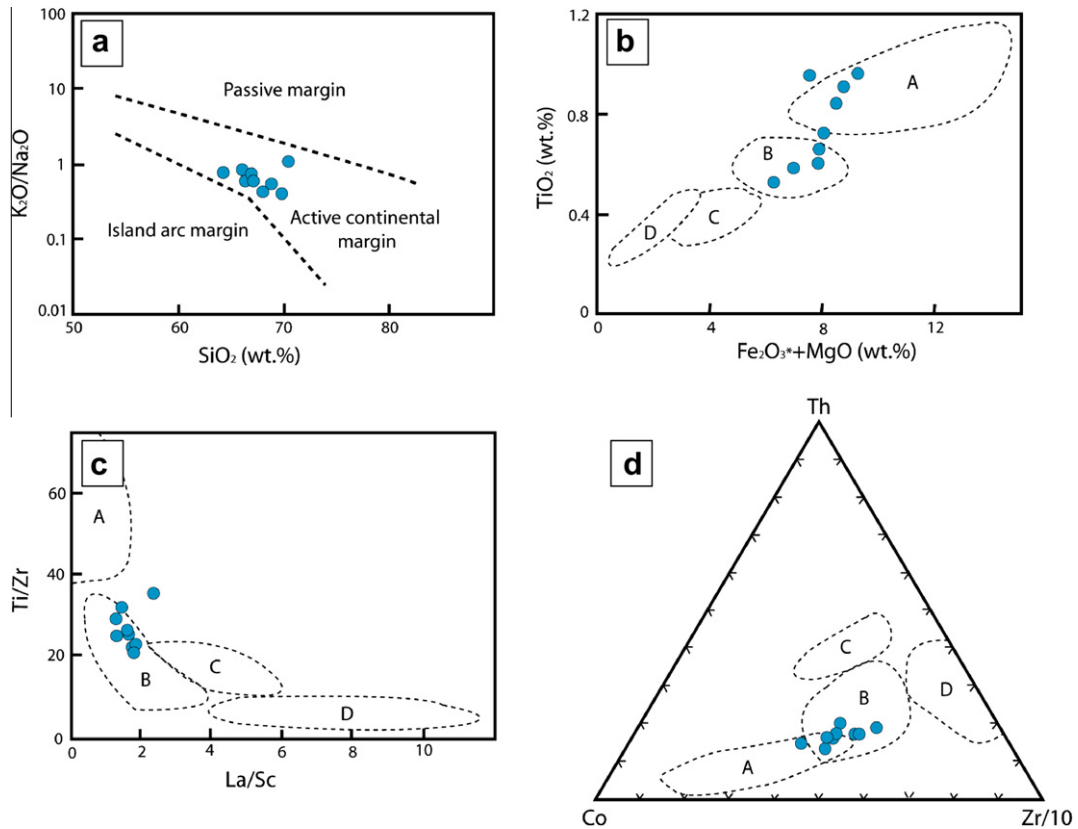


Fig. 9. Tectonic setting discrimination diagrams for Um Hassa greywackes: (a) K_2O/Na_2O versus SiO_2 of Roser and Korsch (1986), (b) TiO_2 versus $Fe_2O_3 + MgO$ of Bhatia (1983), (c) Ti/Zr versus La/Sc of Bhatia and Crook (1986), and (d) Co-Th-Zr ternary diagram of Bhatia and Crook (1986). (Field A is oceanic island arc, field B is continental island arc, field C is active continental margin, and field D is passive continental margin).

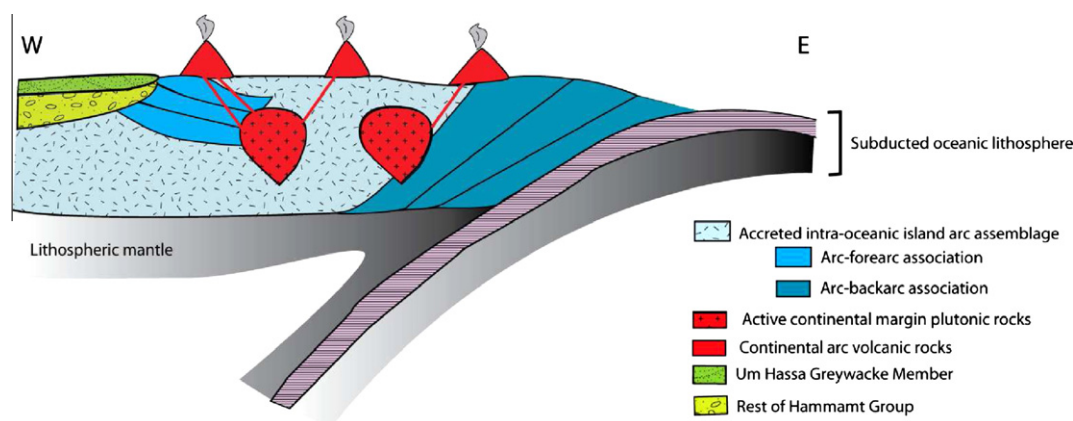


Fig. 10. Tectonic model for the formation of the Hammamat Group at Wadi Hammamat area as inferred from the petrography and geochemistry of the Um Hassa greywacke member.

Eastern Desert can be classified based on their spatial distribution within the orogen and associated structural setting into two main types (Fritz et al., 1996; Fritz and Messner, 1999). The first type, which is a foreland molasse basin, is associated with thrust faults and is located along the western part of the orogen. The second type is related to orogen parallel extension which is related to the Najd strike-slip fault system. The Hammamat Group in their type locality at Wadi Hammamat along Qift-Qusier Road belongs to the first, the foreland molasse, basins.

Foreland basins are classified into two types (Dickinson, 1974). The first type is the peripheral foreland basin, which is formed in the front of fold-and-thrust belts, while the second type is the retroarc foreland basin which is formed in the hinterland side of continental arcs (DeCelles and Giles, 1996). One alternative for the Um Hassa greywackes is that they would have been deposited in a peripheral foreland basin formed during the accretion of the oceanic island arc and ophiolitic materials to the Saharan Craton to the west, during east-dipping subduction. Such a model is similar to the ones proposed during the evolution of the Taconic orogeny in northern Appalachians (Garver et al., 1996) and the evolution of the Grenvillian orogeny in southern Africa (Basson and Watkey, 2003). In favor of the peripheral foreland basin model, the plot of the Um Hassa greywackes in the continental island arc and active continental margin fields on the tectonic discrimination diagrams (Fig. 9) can be interpreted in terms of mixing components from different sources. These sources would have been the passive continental margin sediments derived from the Saharan Craton to the west and the accreted oceanic island arc-ophiolitic rocks from the west. This model is unlikely because of the scarcity of sedimentary lithic fragments compared to the amount of volcanic lithic fragments (Fig. 8c). It is most likely that the Um Hassa greywackes were deposited in a retroarc, rather than a peripheral, foreland basin where the sediments derived mainly from the continental arcs with a contribution from the basement substrate which is composed of island arc and ophiolitic rocks (Fig. 10). Thus, the plot of the Um Hassa greywackes in the continental arc field reflects the chemical characteristics of these volcanic lithic fragments. Such a chemical affinity of the lithic components suggests the deposition of the Hammamat Group at its type locality in a retroarc foreland basin, similar to the tectonic setting of the cordilleran retroarc foreland basins of North America (DeCelles, 2004).

Tectonic contact between the Dokhan Volcanics and Hammamat Group in the Wadi Hammamat area can be attributed to later reactivation of thrust faults in the accreted island arc and ophiolitic materials. This reactivation might have resulted in the folding and cleavage development recorded in the Hammamat sediments. The possibility for the Hammamat Group in the Wadi Hammamat area

of being deposited in piggy-back basins as suggested by Andresen et al. (2009) is less likely. In such basins, sediments are expected to be derived from the accreted arc and ophiolitic thrust sheets rather than being derived from continental arc rocks (Dokhan-type Volcanics). In addition, sediments deposited in piggy-back basins are expected to be severely deformed during thrust reactivation periods. These characteristics match the sediments of Wadi Um Esh, which are located to the east of the Wadi Hammamat area. The sediments of Wadi Um Esh have restricted pebble types, including trondhjemite, fine-grained basic rocks and epidosite, and are intensely deformed (Ries et al., 1983, and reference therein). Deposition of the Um Esh sediments in a restricted piggy-back basin to the east relative to the less deformed, thick Hammamat sediments to the west supports the probability for the Hammamat Group being deposited in a retroarc foreland basin. Unfortunately, the cover of the Hammamat Group by younger Phanerozoic sandstone prevents a detailed study of these sedimentary rocks to the west in order to establish their relationship with the Saharan Metacraton.

7. Conclusion

The petrographic characteristics of the Um Hassa greywackes are consistent with their derivation from mixed sources such as the underlying Um Had Conglomerate Member. In addition to this, the low CIA and $\text{SiO}_2/\text{Al}_2\text{O}_3$ ratios indicate slight weathering of the source rocks and deposition of the fragments close to the source. Limited weathering and transportation of the Um Hassa sediments indicates the reliability of using geochemical characteristics to interpret their provenance.

The geochemistry of the Um Hassa greywackes (low Th/Sc, Zr, Nb, Th/U, and high Cr and Ni), suggests both the Dokhan-type continental arc volcanics and accreted ophiolitic-arc materials are the main sources to the upper part of Hammamat sediments. In the context of the evolution of the Central Eastern Desert, the Um Hassa Greywacke Member at Wadi Hammamat area was deposited in a retroarc foreland basin. This basin formed behind the continental arcs established over a west-dipping subduction zone.

Acknowledgements

Two reviewers (Read Mapeo and anonymous) and the editor (P. Eriksson) are acknowledged for their constructive comments. We thank Dr. Leon Lang for providing us with a copy of the Asran et al. (2005) paper. The revision of the manuscript by Dr. Patricia Corcoran is highly appreciated. This study is a contribution of the

PREA Grant to A. Polat. Support from NSERC Grants of Ali Polat (250978) and Brian Fryer (83117) are greatly appreciated.

References

- Aagaard, P., Jahren, J.S., 1992. Diagenetic illite–chlorite assemblages in arenites. II. Thermodynamic relations. *Clays and Clay Minerals* 40, 547–554.
- Aagaard, P., Jahren, J., Harstad, A.O., Nilsen, O., Ramm, M., 2000. Formation of grain-coating chlorite in sandstones; laboratory synthesized vs. natural occurrences. *Clay Minerals* 35, 261–269.
- Abdel Rahman, Y.M.H., 2004. Geology and mineralizations of the Precambrian rocks at Wadi Hamama area, Central Eastern Desert, Egypt. MSc Thesis, Cairo University, 189pp.
- Abd El-Rahman, Y., Polat, A., Dilek, Y., Fryer, B.J., El-Sharkawy, M., Sakran, S., 2009a. Geochemistry and tectonic evolution of the Neoproterozoic incipient arc-forearc crust in the Fawakhir area, Central Eastern Desert, Egypt. *Precambrian Research* 175, 116–134.
- Abd El-Rahman, Y., Polat, A., Dilek, Y., Fryer, B.J., El-Sharkawy, M., Sakran, S., 2009b. Geochemistry and tectonic evolution of the Neoproterozoic Wadi Ghadir ophiolite, Eastern Desert, Egypt. *Lithos* 113, 158–178.
- Abd El-Wahed, M.A., 2007. Late Pan-African tectonic evolution and strain determinations in the Late Neoproterozoic molasse sediments, Eastern Desert, Egypt: evidence for post-Hammamat compression and transpression. *Egyptian Journal of Geology* 51, 1–39.
- Abu El Ela, A.M., El Bahariya, G.A., 1995. The Hammamat molasse sediments between Wadi Um Esh and Wadi Muweilih, Qift-Quseir Road Region, Central Eastern Desert, Egypt. *Egyptian Journal of Geology* 41, 5–35.
- Akaad, M.K., Noweir, A.M., 1969. Lithostratigraphy of the Hammamat–Um Seleimat District, Eastern Desert, Egypt. *Nature* 223, 284–285.
- Akaad, M.K., Noweir, A.M., 1980. Geology and lithostratigraphy of the Arabian Desert orogenic belt of Egypt between latitudes 25°35' and 26°30'N. *Institute of Applied Geology Bulletin*, Jeddah 3, 127–136.
- Andresen, A., Abu El-Rus, M.A., Myhre, P.L., Boghdady, G.Y., Corfu, F., 2009. U–Pb TIMS age constraints on the evolution of the Neoproterozoic Meatiq Gneiss Dome, Eastern Desert, Egypt. *International Journal of Earth Sciences* 98, 481–497.
- Asran, A.M.H., Azer, M.K., Aboazom, A.S., 2005. Petrological and geochemical investigation of Dokhan volcanics and felsites in Wadi Sodmein area, Central Eastern Desert, Egypt. *Egyptian Journal of Geology* 49, 1–20.
- Basson, I.J., Watkey, M.K., 2003. Tectonic implications from the geochemistry of Mfongosi Group metasediments, Natal metamorphic province, South Africa. *South African Journal of Geology* 106, 265–280.
- Basu, A., Young, S.W., Suttner, L.J., James, W.C., Mack, G.H., 1975. Re-evaluation of the use of undulatory extinction and polycrystallinity in detrital quartz for provenance interpretation. *Journal of Sedimentary Petrology* 45, 873–882.
- Bhatia, M.R., 1983. Plate tectonics and geochemical composition of sandstones. *Journal of Geology* 91, 611–627.
- Bhatia, M.R., Crook, K.A.W., 1986. Trace element characteristics of greywackes and tectonic setting discrimination of sedimentary basins. *Contributions to Mineralogy and Petrology* 92, 181–193.
- Camiré, G.E., Lafleche, M.R., Ludden, J.N., 1993. Archaean metasedimentary rocks from the northwestern Pontiac sub-province of the Canadian Shield: chemical characterization, weathering and modeling of the source areas. *Precambrian Research* 62, 285–305.
- Crook, K.A.W., 1974. Lithogenesis and geotectonics: the significance of the compositional variations in flysch arenites (greywackes). In: Dott, R.H., Shaver, R.H. (Eds.), *Modern and Ancient Geosynclinal Sedimentation*, vol. 19. SEPM Special Publication, pp. 304–310.
- DeCelles, P.G., 2004. Late Jurassic to Eocene evolution of the cordilleran thrust belt and foreland basin system, Western USA. *American Journal of Science* 304, 105–168.
- DeCelles, P.G., Giles, K.A., 1996. Foreland basin systems. *Basin Research* 8, 105–123.
- Dickinson, W.R., 1974. Plate tectonics and sedimentation. *Society of Economic Paleontologists and Mineralogists Special Publication* 22, 1–27.
- Dickinson, W.R., 1985. Interpreting provenance relations from detrital modes of sandstones. In: Zuffa, G.G. (Ed.), *Provenance of Arenites*. D. Reidel Publishing Company, Dordrecht, pp. 333–361.
- Dickinson, W.R., Beard, L.S., Brakenridge, G.R., Erjavec, J.L., Ferguson, R.C., Inman, K.F., Knepp, R.A., Lindberg, F.A., Ryberg, P.T., 1983. Provenance of North American Phanerozoic sandstones in relation to tectonic setting. *Geological Society of America Bulletin* 94, 222–235.
- Dickinson, W.R., Suczek, C.A., 1979. Plate tectonics and sandstone compositions. *American Association of Petroleum Geologists Bulletin* 63, 2164–2182.
- El-Bouseily, A.M., 1986. On trondhjemitic pebbles from the late Pan-African Um Had conglomerate, Eastern Desert Egypt. *Journal of African Earth Sciences* 5, 471–480.
- El Gaby, S., El-Nady, O., Khudeir, A., 1984. Tectonic evolution of the basement complex in the Central Eastern desert of Egypt. *Geologische Rundschau* 73, 1019–1036.
- Eliwa, H.A., Kimura, J.I., Itaya, T., 2006. Late Neoproterozoic Dokhan volcanic rocks, northern Eastern Desert, Egypt. *Precambrian Research* 151, 31–52.
- El Kalioubi, B., 1996. Provenance, tectonic setting and geochemical characteristics of the Hammamat molasse sediments around Um Had pluton, Eastern Desert, Egypt. *MERC Ain Shams University. Earth Science Series* 10, 75–88.
- Engel, A.E.J., Dixon, T.H., Stern, R.J., 1980. Late Precambrian evolution of Afro-Arabian crust from ocean-arc to craton. *Geological Society of American Bulletin* 91, 385–411.
- Fedo, C.M., Nesbitt, H.M., Young, G.M., 1995. Unraveling the effects of potassium metasomatism in sedimentary rocks and paleosols, with implications for paleoweathering conditions and provenance. *Geology* 23, 921–924.
- Fedo, C.M., Young, G.M., Nesbitt, H.M., Hancher, J.M., 1997. Potassic and sodic metasomatism in the Southern province of Canadian Shield: evidence from paleoproterozoic serpent formation, Huronian supergroup, Canada. *Precambrian Research* 84, 17–36.
- Fowler, A., El Kalioubi, B., 2004. Gravitational collapse origin of shear zones, foliation and linear structures in the Neoproterozoic cover nappes, Eastern Desert, Egypt. *Journal of African Earth Sciences* 38, 23–40.
- Fowler, A., Osman, A.F., 2001. Gneiss-cored interference dome association with two phases of late Pan-African thrusting in the central Eastern Desert, Egypt. *Precambrian Research* 108, 17–43.
- Fritz, H., Messner, M., 1999. Intramontane basin formation during oblique convergence in the Eastern desert of Egypt: magmatically versus tectonically induced subsidence. *Tectonophysics* 315, 145–162.
- Fritz, H., Wallbrecher, E., Khudeir, A.A., Abu El Ela, F., Dallmeyer, D.R., 1996. Formation of Neoproterozoic metamorphic core complexes during oblique convergence (Eastern Desert, Egypt). *Journal of African Earth Sciences* 23, 311–329.
- Garver, J.I., Royce, P.R., Smick, T.A., 1996. Chromium and nickel in shale of the Taconic Foreland: a case study for the provenance of the fine-grained sediments with an ultramafic source. *Journal of Sedimentary Research* 66, 100–106.
- Greiling, R.O., Abdeen, M.M., Dardir, A.A., El Akhal, H., El Ramly, M.F., Kamal El Din, G.M., Osman, A.F., Rashwan, A.A., Rice, A.H.N., Sadek, M.F., 1994. A structural synthesis of the Proterozoic Arabian–Nubian Shield in Egypt. *Geologie Rundschau* 83, 484–501.
- Grigsby, J.D., 2001. Origin and growth mechanism of authigenic chlorite in sandstones of the Lower Vicksburg Formation, south Texas. *Journal of Sedimentary Research* 71, 27–36.
- Grothaus, B.T., Ehrlich, R., Eppler, D.T., 1979. Facies analysis of the Hammamat sediments, Eastern Desert, Egypt. In: 5th Conference on African Geology, Cairo, *Annals of the Geological Survey of Egypt*, vol. 9, pp. 564–590.
- Hendrix, M.S., 2000. Evolution of Mesozoic sandstone compositions, southern Junggar, northern Tarim, and western Turpan Basin, northwest China: a detrital record of the ancestral Tian Shan. *Journal of Sedimentary Research* 70, 520–532.
- Heikal, M.T.S., 2003. Petrogenesis of gneissic granitoids across Qift-Quseir road, Central Eastern Desert of Egypt: petrological and geochemical constraints. In: 5th International Conference on the Geology of the Middle East, pp. 253–276.
- Hiscott, R.N., 1984. Ophiolitic source rocks for Taconic-age flysch: trace element evidence. *Geological Society of American Bulletin* 95, 1261–1267.
- Holail, H.M., Moghazi, A.M., 1998. Provenance, tectonic setting and geochemistry of greywackes and siltstones of the Late Precambrian Hammamat Group, Egypt. *Sedimentary Geology* 116, 227–250.
- Jenner, G.A., Longerich, H.P., Jackson, S.E., Fryer, B.J., 1990. ICP-MS – a powerful tool for high-precision trace-element analysis in earth sciences: evidence from analysis of selected U.S.G.S. reference samples. *Chemical Geology* 83, 133–148.
- Johnson, P.R., Woldehaimanot, B., 2003. Development of the Arabian–Nubian Shield: perspectives on accretion and deformation in the northern East African Orogen and the assembly of Gondwana. In: Yoshida, M., Windley, B.F., Dasgupta, S. (Eds.), *Proterozoic East Gondwana: Super Continent Assembly and Break-Up*, vol. 206. Geological Society of London Special Publications, pp. 289–325.
- McLennan, S.M., Bock, B., Hemming, S.R., Hurowitz, J.A., Lev, S.M., McDaniel, D.K., 2003. The role of provenance and sedimentary processes in the geochemistry of sedimentary rocks. In: Lentz, D.R. (Ed.), *Geochemistry of Sediments and Sedimentary Rocks: Evolution Considerations to Mineral Deposit-Forming Environments*, vol. 4. Geological Association of Canada, *GeoText*, pp. 7–38.
- McLennan, S.M., Hemming, S., McDaniel, D.K., Hanson, G.N., 1993. Geochemical approaches to sedimentation, provenance and tectonics. In: Johnson, M.J., Basu, A. (Eds.), *Processes Controlling the Composition of Clastic Sediments*, vol. 284. Geological Society of America, Special Paper, pp. 21–40.
- McLennan, S.M., Taylor, S.R., McCulloch, M.T., Maynard, J.B., 1990. Geochemical and Nd–Sr isotopic composition of deep sea turbidites: crustal evolution and plate tectonic association. *Geochimica et Cosmochimica Acta* 40, 1537–1551.
- Middleton, G.V. (Ed.), 2003. *Encyclopedia of Sediments and Sedimentary Rocks*. Springer-Verlag.
- Nesbitt, H.W., 2003. Petrogenesis of siliciclastic sediments and sedimentary rocks. In: Lentz, D.R. (Ed.), *Geochemistry of Sediments and Sedimentary Rocks: Evolution Considerations to Mineral Deposit-Forming Environments*, vol. 4. Geological Association of Canada, *GeoText*, pp. 39–51.
- Nesbitt, H.W., Young, G.M., 1982. Early Proterozoic climates and plate motions inferred from major element chemistry of lutites. *Nature* 299, 715–717.
- Nesbitt, H.W., Young, G.M., 1984. Prediction of some weathering trends of plutonic and volcanic rocks based on thermodynamic and kinetic considerations. *Geochimica et Cosmochimica Acta* 48, 1423–1534.
- Nesbitt, H.W., Young, G.M., 1989. Formation and diagenesis of weathering profiles. *Journal of Geology* 97, 129–147.
- Nesbitt, H.W., Young, G.M., 1996. Petrogenesis of sediments in the absence of chemical weathering: effects of the abrasion and sorting on bulk composition and mineralogy. *Sedimentology* 43, 341–358.
- Osman, A.F., El Kalioubi, B., Gaafar, A.Sh., El Ramly, M.F., 2001. Provenance, geochemistry and tectonic setting of Neoproterozoic molasse-type sediments,

- Northern Eastern Desert, Egypt. *Annals of the Geological Survey of Egypt* 24, 93–114.
- Pettijohn, F.G., Potter, P.D., Siever, R., 1972. *Sand and Sandstone*. Springer-Verlag, New York.
- Ries, A.C., Shackleton, R.M., Graham, R.H., Fitches, W.R., 1983. Pan-African structures, ophiolites and mélanges in the Eastern Desert of Egypt: a traverse at 26°N. *Journal of Geological Society* 140, 75–95.
- Roser, B.P., Korsch, R.J., 1986. Determination of tectonic setting of sandstone–mudstone suites using SiO₂ and K₂O/Na₂O ratio. *Journal of Geology* 94, 635–650.
- Roser, B.P., Korsch, R.J., 1988. Provenance signatures of sandstone–mudstone suites determined using discrimination function analysis of major-element data. *Chemical Geology* 67, 119–139.
- Roser, B.P., Korsch, R.J., 1999. Geochemical characterization, evolution and source of Mesozoic accretionary wedge: the Torlesse terrane, New Zealand. *Geological Magazine* 136, 493–512.
- Schwab, F.L., 1975. Framework mineralogy and chemical composition of continental margin-type sandstone. *Geology* 3, 487–490.
- Shalaby, K., Stüwe, H., Fritz, F., Makroum, F., 2006. The El Mayah molasse basin in the Eastern Desert of Egypt. *Journal of African Earth Sciences* 45, 1–15.
- Stern, R.J., 1994. Arc assembly and continental collision in the Neoproterozoic East African Orogen: implications for the consolidation of Gondwanaland. *Annual Review of Earth and Planetary Sciences* 22, 319–351.
- Sun, S.-S., McDonough, W.F., 1989. Chemical and systematic of oceanic basalts: implications for mantle composition and processes. In: Saunders, A.D., Norry, M.J. (Eds.), *Magmatism in Ocean Basins*, vol. 42. Geological Society of London, Special Publication, pp. 313–345.
- Taylor, S.T., McLennan, S.M., 1985. *The Continental Crust: its Composition and Evolution*. Blackwell Scientific, Oxford.
- Whetten, J.T., Hawkins Jr, J.W., 1970. Diagenetic origin of greywacke matrix minerals. *Sedimentology* 15, 347–361.
- Wilde, S.A., Youssef, K., 2001. SHRIMP U–Pb dating of detrital zircons from Hammamat Group at Gebel Um Tawat, Northern-Eastern Desert, Egypt. *Gondwana Research* 4, 202–206.
- Wilde, S.A., Youssef, K., 2002. A re-evaluation of the origin and setting of the late Precambrian Hammamat Group based on SHRIMP–U–Pb dating of detrital zircons from Gebel Umm Tawat, North Eastern Desert, Egypt. *Journal of Geological Society London* 159, 595–604.
- Worden, R.H., Burley, S.D., 2003. Sandstone diagenesis: the evolution of sand to stone. In: Burley, S.D., Worden, R.H. (Eds.), *Sandstone Diagenesis: Recent and Ancient*, vol. 4. International Association of Sedimentologists Reprint, pp. 3–44.
- Zhang, K.-J., 2004. Secular geochemical variations of the Lower Cretaceous siliciclastic rocks from central Tibet (China) indicate a tectonic transition from continental collision to back-arc rifting. *Earth and Planetary Science Letters* 229, 73–89.
- Zhang, K.-J., Li, B., Wei, Q.-G., Gai, J.-X., Zhang, Y.-X., 2008. Proximal provenance of the western Songpan-Ganzi turbidite complex (Late Triassic, eastern Tibetan plateau): implication for the tectonic amalgamation of China. *Sedimentary Geology* 208, 36–44.